Optics Communications 281 (2008) 5830–5837

Contents lists available at ScienceDirect

Optics Communications

journal homepage: www.elsevier.com/locate/optcom

# Mechanically controlled bandgap in cholesteric elastomers

Tania Espinosa-Ortega, Juan Adrian Reyes *

*Física Química, Instituto de Física, Universidad Nacional Autónoma de México, México, D.F. 04510, Mexico*

ARTICLE INFO

*Article history:*
Received 15 September 2007
Received in revised form 26 July 2008
Accepted 6 August 2008

ABSTRACT

The propagation of an electromagnetic wave traveling in a chiral elastomer under the influence of an externally induced mechanical strain, applied parallel to the helical axis, is investigated. We write and solve Maxwell equations in the Oseen reference system by performing a numerical integration to find the transmission and reflection coefficients as a function of the mechanical elongation and the incidence angles. Then, the transmittances and the reflectances are calculated and analyzed. A mechanically controlled circular Bragg phenomenon is observed for which the bandwidth and the central wavelength are significantly modified. It is also shown that the reflection bandgap blue-shifts versus the incidence angles, as happens in absence of strain.



## 1. Introduction

The Bragg phenomenon is exhibited by a layer of a material whose electromagnetic constitutive properties are periodically nonhomogeneous in the thickness direction. Its keynote is a very high reflectance in a certain wavelength-interval, on the condition the slab is thick enough to have an adequate large number of periods. This phenomenon is commonly utilized to make dielectric mirrors in optics [1].

Periodicity arises from structural chirality which means a helicoidal variation of anisotropy along a fixed axis. To illustrate structurally chiral materials (SCMs) we can mention cholesteric liquid crystals [2,3], chiral sculptured thin films [4] and chiral elastomers [5]. As the periodicity arises from structural chirality, incident electromagnetic plane waves of left- and right-circular polarization (LCP and RCP) states are reflected and transmitted differently in the Bragg wavelength-regime, and the Bragg phenomenon is then called the *circular* Bragg phenomenon (CBP). Exhibition of the CBP by cholesteric liquid crystals and chiral sculptured thin films underlies their use as circular-polarization rejection filters in optics [2,4].

Control of the CBP is very desirable for tuning the Bragg regime as well as for switching applications. One way would be to use SCMs that are electro-optically controlled systems. This possibility, also suggested by the fabrication of electro-optic filters [6], was proposed and theoretically examined in a recent publication [7]. It was indeed found that a dc electric field creates a Bragg regime even when the SCM properties were such that a regime would not exist in the absence of the electric field [8].

Cholesteric elastomers are formed by monomers of liquid crystals cross-linked to polymeric chains; this union produces a flexible material whose molecular order is similar to cholesteric liquid crystals with the advantage that in this new material it is possible to change the optical properties by means of macroscopic deformations [5]. The study of the optical properties of these materials have recently grown due to the achievement managed by Kim and Finkelmann who found a procedure to obtain monodomain nematic and cholesteric elastomers [9]. Furthermore, a more promising method for generating films of cholesteric elastomers by cross-linking under UV irradiation has been recently developed [10].

For normally incident light on a contracted cholesteric film, a blue-shift of the photonic stop band has been experimentally and theoretically found [11]. A numerical study of the circularly polarized reflectances due to an elastomer slab elongated by the influence of a uniaxial transverse strain, was done [12]. Nested optical bandgaps were found for left- and right-circularly polarized light. Here, we propose to use a cholesteric elastomer subjected to an externally imposed deformation for tuning the circular Bragg regime exhibited by the elastomer in the absence of the strain.

The outline of this paper is as follows: In Section 2 we discuss the elastic model for describing a cholesteric elastomer slab subjected to a mechanical strain applied along the helix axis of the elastomer. Section 3 contains a brief description of the optical permittivity matrix of a chiral material, and the Oseen transformation is employed to derive an analytical expression for the central wavelength of the band reflection in the Bragg regime. Section 4 accounts for the numerical results and discussions concerning the mechanical strain in relation to the exhibition of the CBP.

## 2. Elastic energy

Let us consider a monodomain cholesteric elastomer subjected to the action of a longitudinal elongation. The microscopic

* Corresponding author.
*E-mail address:* adrian@fisica.unam.mx (J.A. Reyes).

0030-4018/$ - see front matter © 2008 Elsevier B.V. All rights reserved.
doi:10.1016/j.optcom.2008.08.019

statistical–mechanical theory of rubber elasticity leads to the classical nematic rubber elasticity energy density so called the trace formula when anisotropy is taken into account [5]. It is given by

$$F = \frac{1}{2}\mu \mathrm{Tr}[\mathbf{l}_0 \cdot \eta^T \cdot \mathbf{l}^{-1} \cdot \eta], \tag{1}$$

where $\mu = n_s \kappa_B T$ is the rubber shear modulus, $n_s$ is the number of chains strands per unit of volume, $\kappa_B$ is the Boltzmann constant, $T$ is the temperature, Tr stands for the trace of the tensor and the local step-length tensors for a locally uniaxial medium are

$$\mathbf{l}_0 = l_\perp(\delta + (r-1)\mathbf{n}_0\mathbf{n}_0), \tag{2}$$

$$\mathbf{l}^{-1} = l_\perp(\delta + (1/r-1)\mathbf{n}\mathbf{n}), \tag{3}$$

where $r = l_\parallel/l_\perp$ is the anisotropy ratio.

In deriving Eq. (1) the entanglements, finite extensibility and semi-softness have been ignored. Here, the director corresponding to the initial configuration is denoted by

$$\hat{\mathbf{n}}_0 = (\cos\phi_0, \sin\phi_0, 0), \tag{4}$$

where the angle $\phi_0 = q_0 z$ has a helix wave number $q_o = 2\pi/p$ and a spatial periodicity or pitch $p$. This is determined by the concentration and the helical twisting power of the chiral constituents [13]. Usually the pitch is of the same order as the wavelength. After the deformation the director is aligned along the surface of a cone, as shown in Fig. 1, which can be described by

$$\hat{\mathbf{n}} = (\sin\alpha\cos\phi, \sin\alpha\sin\phi, \cos\alpha), \tag{5}$$

where $\phi = qz$ and $\alpha$ are the azimuthal and polar angles.

When the elastomer is submitted to an elongation, a selected chain's end-to-end vector $\mathbf{R}$ is assumed to deform proportionally to the body's deformation. The proportionality factor is given by the deformation tensor $\eta$ which in the case of an expansion parallel to the helix axis, $\eta$ has the form [5]:

$$\eta = \begin{pmatrix} \frac{1}{\sqrt{\eta}} & 0 & \eta_{xz}(z) \\ 0 & \frac{1}{\sqrt{\eta}} & \eta_{yz}(z) \\ 0 & 0 & \eta \end{pmatrix}, \tag{6}$$

where we have taken $\eta_{zz} = \eta$. This expression preserves the volume since by construction $Det\eta = 1$ is fulfilled. There is no compatibility inconsistency due to the $z$-dependence of the elongations $\eta_{xz}(z)$ and $\eta_{yz}(z)$. In contrast, the $z$-dependence of their conjugate strains $\eta_{zx}(z)$ and $\eta_{zy}(z)$ would lead to compatibility mismatch as for instance the expression: $\partial\eta_{zx}(z)/\partial z = \partial\eta_{zz}(z)/\partial x$ cannot be fulfilled unless we set $\partial\eta_{zx}(z)/\partial z = 0$. Finally, $\eta_{xy}(z)$ and $\eta_{yx}(z)$ could exist but numerical tests suggest that it is not possible [14]. The two shear strains $\eta_{xz}(z)$ and $\eta_{yz}(z)$ should be proportional to each other so that they are part of a shear in the plane of $\hat{\mathbf{n}}_0$ and $\hat{\mathbf{n}}$. These two shears help to accommodate the rotation of the chain distributions in such way to keep the elastic energy low, while the director $\hat{\mathbf{n}}$ turns. In other words, the network deforms to allow rotate $\hat{\mathbf{n}}$ practically without any energy penalty. All physical dimensions in the deformed sample are assumed to scale by the affine strain as $z \to z/\eta$ resulting in the corresponding expansion of the cholesteric pitch $q = \frac{q_o}{\eta}$.

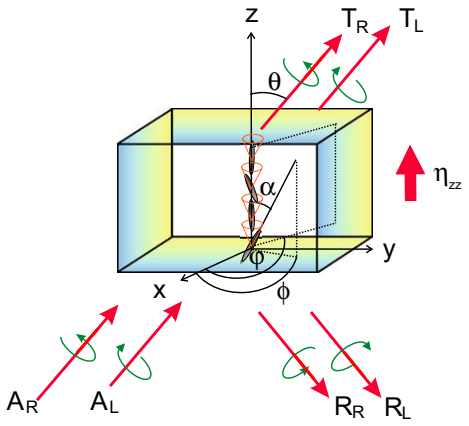


**Fig. 1.** Schematic plot of an elastomer slab elongated along the $z$-direction. The light incidence angles $\theta$ and $\varphi$ and the helix angles $\phi$ and $\alpha$ are shown. $A_{L,R}$ are the incident left- and right-circularly polarized amplitudes, $R_{L,R}$ are the corresponding reflection amplitudes and $T_{L,R}$ are the corresponding transmitted amplitudes.

Using the above equations, the free energy for an elastomer under mechanical strain can be obtained. Thus, by minimizing the free Helmholtz energy first with respect to the strains $\eta_{xz}(z)$ and $\eta_{yz}(z)$, and then with respect to $\chi$, where $\chi = \frac{\pi}{2} - \alpha$, we obtain

$$\chi(\eta) = \arcsin\sqrt{\frac{\eta^{3/2}-1}{r-1}}. \tag{7}$$

It can be inferred from this equation that the nematic's vector will be totally aligned with the $z$-axis for the critical longitudinal stress which is equal to

$$\eta_M = r^{2/3}. \tag{8}$$

It should be mentioned that Eq. (7) is only valid in the interval $1 \leqslant \eta \leqslant \eta_M$ since a uniaxial compression ($\eta < 1$) parallel to the helix axis leaves the helical structure unchanged. Also, an extension beyond $\eta_M$ does not change the value of $\chi$ any further.

Eq. (7) provides an expression to determine the director vector $\hat{\mathbf{n}}$ which allows us to find the dielectric tensor of the elastomer: $\epsilon = \epsilon_\perp \delta_{ij} + \epsilon_a \hat{\mathbf{n}}\hat{\mathbf{n}}$, where $\epsilon_a = \epsilon_\parallel - \epsilon_\perp$, is the dielectric anisotropy, $\epsilon_\parallel$ and $\epsilon_\perp$ are the dielectric constants parallel and perpendicular to the director $\hat{\mathbf{n}}$.

## 3. Electromagnetic propagation

### 3.1. Boundary conditions

We consider the case where a circularly polarized electromagnetic wave impinges an elastomer slab of thickness $L$, situated in the region $0 < z < L$ which is surrounded by two half spaces of vacuum with the $z$-axis parallel to the helical axis.

In the half space $z < 0$, we assume both, an incident and a reflected circularly polarized waves as shown in Fig. 1, which can be expressed as a linear combination of a left- and right-circularly polarized wave which are given by

$$\mathbf{E}(\mathbf{r}) = (A_R\mathbf{n}_{-1} + A_L\mathbf{n}_{+1})e^{i\mathbf{k}_1\cdot\mathbf{r}} + (R_R\mathbf{n}_{-2} + R_L\mathbf{n}_{+2})e^{i\mathbf{k}_2\cdot\mathbf{r}}, \tag{9}$$

$$\mathbf{H}(\mathbf{r}) = \frac{1}{\mu_0\omega}\left[\mathbf{k}_1 \times (A_R\mathbf{n}_{-1} + A_L\mathbf{n}_{+1})e^{i\mathbf{k}_1\cdot\mathbf{r}} + \mathbf{k}_2 \times (R_R\mathbf{n}_{-2} + R_L\mathbf{n}_{+2})e^{i\mathbf{k}_2\cdot\mathbf{r}}\right], \tag{10}$$

where $\omega$ is the frequency of the wave, $\mathbf{k}_i = k_x\mathbf{u}_x + k_y\mathbf{u}_y - (-1)^i k_z\mathbf{u}_z$ ($i = 1, 2$) are the forward and backward wave vectors, $\mu_o$ is the permeability of the vacuum, $A_{L,R}$ the incident left- and right-circularly polarized amplitudes, $R_{L,R}$ the corresponding reflection amplitudes and the unit vectors

$$\mathbf{n}_{\pm j} = \frac{(-1)^{j+1}}{\sqrt{2}}\left(\frac{[\mathbf{u}_z \times \mathbf{k}_j] \times \mathbf{k}_j}{|\mathbf{u}_z \times \mathbf{k}_j|k_j} \pm i\frac{\mathbf{u}_z \times \mathbf{k}_j}{|\mathbf{u}_z \times \mathbf{k}_j|}\right), \tag{11}$$

where $(\mathbf{u}_x, \mathbf{u}_y, \mathbf{u}_z)$ is the triad of Cartesian unit vectors. Here $\mathbf{u}_z \times \mathbf{k}_1$ is a normal vector to the incidence plane whereas $[\mathbf{u}_z \times \mathbf{k}_1] \times \mathbf{k}_1$ is a vector on the incidence plane and perpendicular to $\mathbf{k}_1$. Thus, both vectors form a complete base for expanding the linearly polarized incident electric field $\mathbf{E}(\mathbf{r})$, while $\mathbf{n}_{+1}$, $\mathbf{n}_{-1}$ play the same role for a circularly polarized field. A similar discussion is valid for the base of vectors: $\{\mathbf{n}_{+2}, \mathbf{n}_{-2}\}$ corresponding to the reflected wave. In the region $z > L$, we write the transmitted fields as

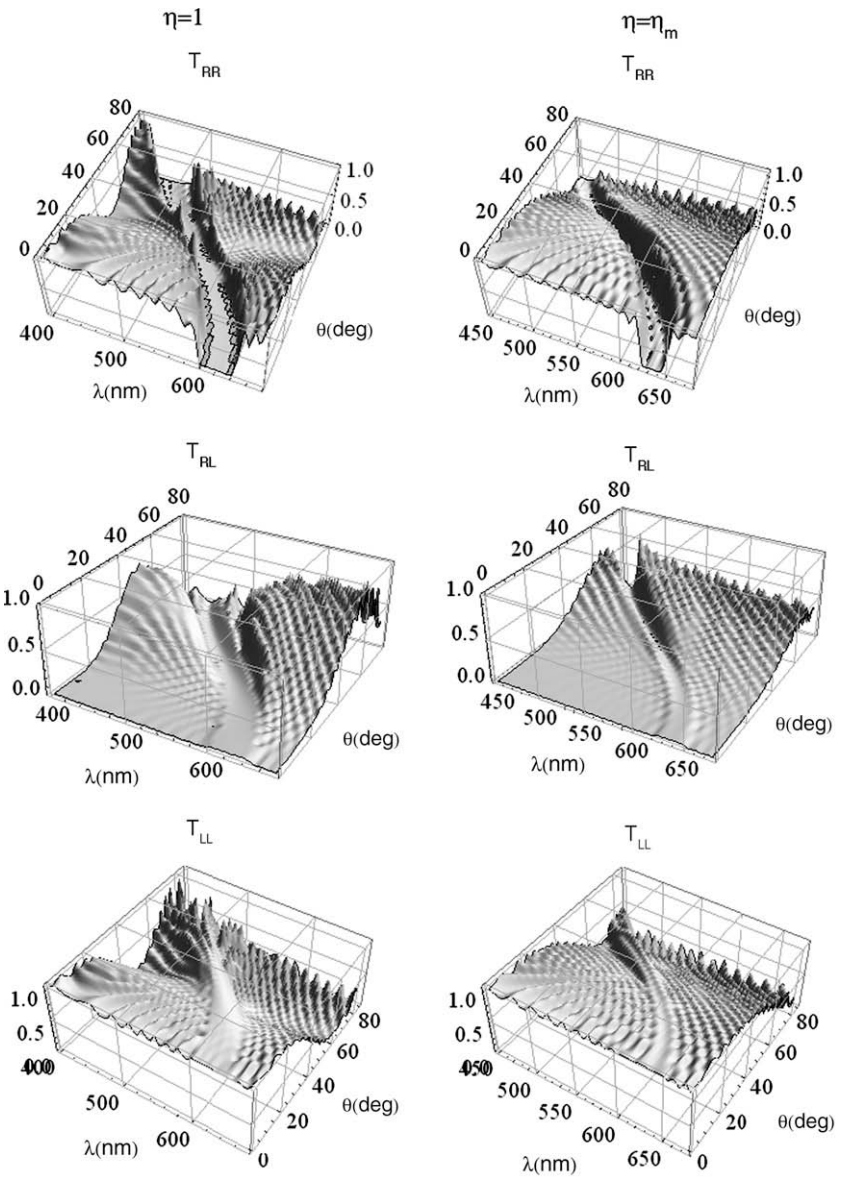


**Fig. 2.** Transmittances versus the wavelength $\lambda$ and the incidence angle $\theta$ for the elongations $\eta = 1$ and $\eta = \eta_m$.

$$\mathbf{E}(\mathbf{r}) = (T_{\mathrm{R}}\mathbf{n}_{-1} + T_{\mathrm{L}}\mathbf{n}_{+1})\mathrm{e}^{\mathrm{i}\mathbf{k}_1\cdot\mathbf{r}} + (B_{\mathrm{R}}\mathbf{n}_{-2} + B_{\mathrm{L}}\mathbf{n}_{+2})\mathrm{e}^{\mathrm{i}\mathbf{k}_2\cdot\mathbf{r}}, \tag{12}$$

$$\mathbf{H}(\mathbf{r}) = \frac{1}{\mu_0\omega}\left[\mathbf{k}_1 \times (T_{\mathrm{R}}\mathbf{n}_{-1} + T_{\mathrm{L}}\mathbf{n}_{+1})\mathrm{e}^{\mathrm{i}\mathbf{k}_1\cdot\mathbf{r}} + \mathbf{k}_2 \times (B_{\mathrm{R}}\mathbf{n}_{-2} + B_{\mathrm{L}}\mathbf{n}_{+2})\mathrm{e}^{\mathrm{i}\mathbf{k}_2\cdot\mathbf{r}}\right], \tag{13}$$

where $T_{\mathrm{L,R}}$ are the corresponding transmitted amplitudes whereas $B_{\mathrm{R,L}}$ are also incident amplitudes but coming from the region $z > L$. Nevertheless, in what follows we shall take $B_{\mathrm{R}} = B_{\mathrm{L}} = 0$.

It is convenient to define a four-dimensional vector $\boldsymbol{\Phi}(z)$ containing the tangential components $E_x(z)$, $E_y(z)$, $H_x(z)$ and $H_y(z)$ of the electric and magnetic field, respectively, as

$$\boldsymbol{\Phi}(z) = \begin{pmatrix} E_x(z) \\ E_y(z) \\ H_x(z) \\ H_y(z) \end{pmatrix}. \tag{14}$$

Using Eqs. (9), (10), (12) and (13), we can express the tangential components outside of the elastomer as

$$\boldsymbol{\Phi}(0) = \mathbf{Q}\cdot\begin{pmatrix} A_{\mathrm{L}} \\ R_{\mathrm{L}} \\ A_{\mathrm{R}} \\ R_{\mathrm{R}} \end{pmatrix}, \quad \boldsymbol{\Phi}(L) = \mathbf{A}(L)\cdot\mathbf{Q}\cdot\begin{pmatrix} T_{\mathrm{L}} \\ 0 \\ T_{\mathrm{R}} \\ 0 \end{pmatrix}, \tag{15}$$

where the matrices $\mathbf{Q}$ and $\mathbf{A}(L)$ are defined by

$$\mathbf{Q} = \frac{1}{\sqrt{2}\sqrt{k_x^2 + k_y^2}}\begin{pmatrix} \frac{-\mathrm{i}kk_y + k_xk_z}{k} & \frac{\mathrm{i}kk_y + k_xk_z}{k} & \frac{\mathrm{i}kk_y + k_xk_z}{k} & \frac{k_xk_z - \mathrm{i}kk_y}{k} \\ \frac{\mathrm{i}kk_x + k_yk_z}{k} & \frac{k_yk_z - \mathrm{i}kk_x}{k} & \frac{-\mathrm{i}kk_x + k_yk_z}{k} & \frac{\mathrm{i}kk_x + k_yk_z}{k} \\ \frac{-k_yk - \mathrm{i}k_xk_z}{\mu_0\omega} & \frac{k_yk - \mathrm{i}k_xk_z}{\mu_0\omega} & \frac{-k_yk + \mathrm{i}k_xk_z}{\mu_0\omega} & \frac{k_yk + \mathrm{i}k_xk_z}{\mu_0\omega} \\ \frac{k_xk - \mathrm{i}k_yk_z}{\mu_0\omega} & \frac{-k_xk - \mathrm{i}k_yk_z}{\mu_0\omega} & \frac{k_xk + \mathrm{i}k_yk_z}{\mu_0\omega} & \frac{-k_xk + \mathrm{i}k_yk_z}{\mu_0\omega} \end{pmatrix} \tag{16}$$

with $k = \sqrt{k_x^2 + k_y^2 + k_z^2}$ and

$$\mathbf{A}(L) = \begin{pmatrix} \mathrm{e}^{\mathrm{i}k_zL} & 0 & 0 & 0 \\ 0 & \mathrm{e}^{-\mathrm{i}k_zL} & 0 & 0 \\ 0 & 0 & \mathrm{e}^{\mathrm{i}k_zL} & 0 \\ 0 & 0 & 0 & \mathrm{e}^{-\mathrm{i}k_zL} \end{pmatrix}. \tag{17}$$

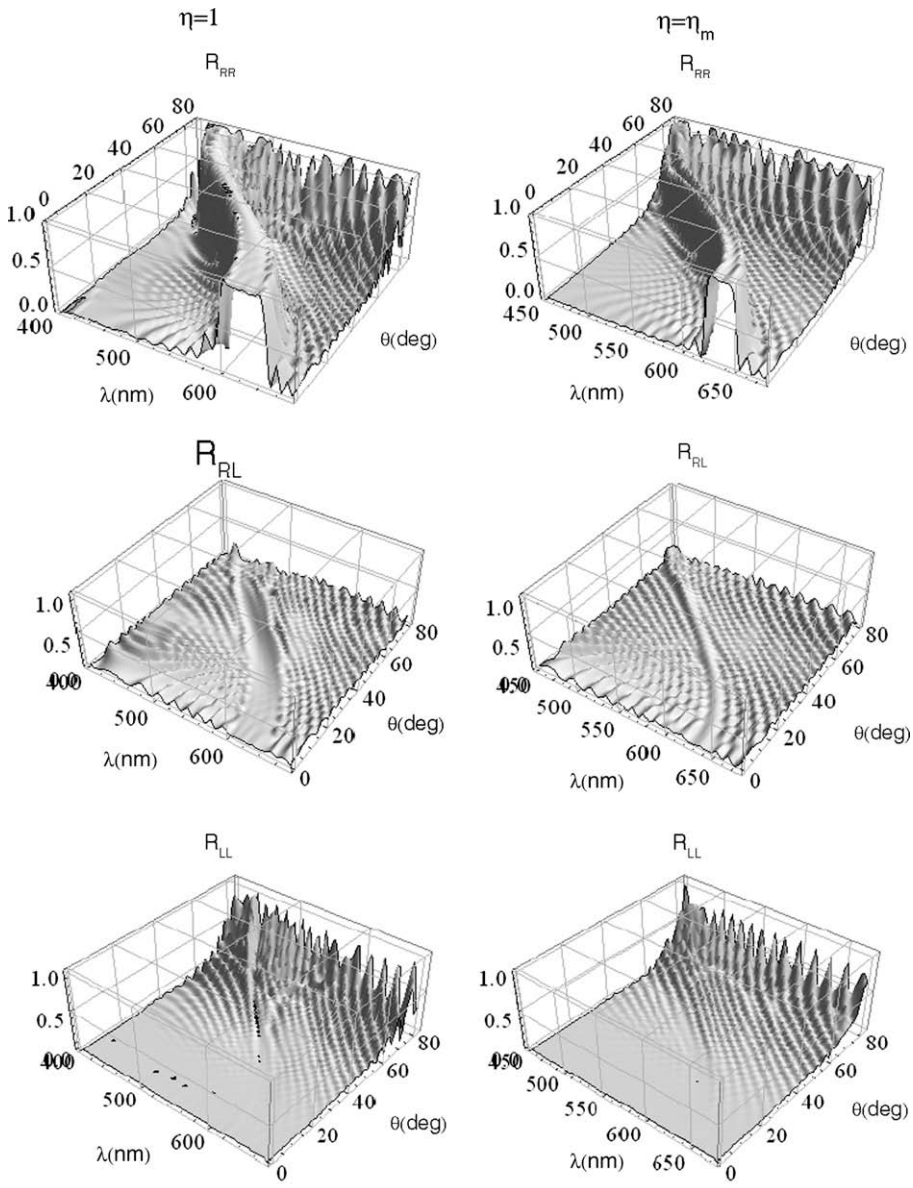


**Fig. 3.** The same as Fig. 2 but for reflectances.

Notice that the expression for normal incidence is obtained upon the consecutive application of the limits: $k_y \to 0$ and $k_x \to 0$. This reduces $\mathbf{Q}$ to the following result

$$\mathbf{Q}_n = \frac{1}{\sqrt{2}} \begin{pmatrix} 1 & 1 & 1 & 1 \\ \mathrm{i} & -\mathrm{i} & -\mathrm{i} & \mathrm{i} \\ -\mathrm{i}\gamma & -\mathrm{i}\gamma & \mathrm{i}\gamma & \mathrm{i}\gamma \\ \gamma & -\gamma & \gamma & -\gamma \end{pmatrix}, \tag{18}$$

where $\gamma = \sqrt{\epsilon_o/\mu_o}$ and $\epsilon_o$ are the impedance and permittivity of the vacuum.

If $\mathbf{U}$ is the transfer matrix of the elastomer slab defined by $\boldsymbol{\Psi}(L) = \mathbf{U} \cdot \boldsymbol{\Psi}(0)$, that we shall derive in next section, and $\boldsymbol{\Psi}$ is defined in similar way as in Eq. (14) but inside the elastomer, then we have

$$\begin{pmatrix} T_L \\ 0 \\ T_R \\ 0 \end{pmatrix} = \mathbf{T}(z) \cdot \begin{pmatrix} A_L \\ R_L \\ A_R \\ R_R \end{pmatrix}, \tag{19}$$

where the transfer matrix for the whole system is given by

$$\mathbf{T}(L) = \mathbf{A}^{-1}(L) \cdot \mathbf{Q}^{-1} \cdot \mathbf{U} \cdot \mathbf{Q}. \tag{20}$$

Here, we have used the continuity of the tangential field components [15] expressed by the conditions: $\boldsymbol{\Psi}(0) = \boldsymbol{\Phi}(0)$ and $\boldsymbol{\Psi}(L) = \boldsymbol{\Phi}(L)$.

Solving the above system for the reflected and transmitted amplitudes, we can obtain the scattering matrix, which gives rise to the relation between the entering and outgoing amplitudes:

$$\begin{pmatrix} T_R \\ T_L \\ R_R \\ R_L \end{pmatrix} = \begin{pmatrix} t_{RR} & t_{RL} \\ t_{RL} & t_{LL} \\ r_{RR} & r_{RL} \\ r_{RL} & r_{LL} \end{pmatrix} \cdot \begin{pmatrix} A_R \\ A_L \end{pmatrix}, \tag{21}$$

where $t_{nm}$ and $r_{nm}$, $(n, m = R, L)$ are the transmission and reflection coefficients. The co-polarized transmittances are denoted by $T_{nn} = |t_{nn}|^2$ and the cross-polarized ones by $T_{nm} = |t_{nm}|^2$ with $n \neq m$; and similarly for the reflectances. These quantities are func-

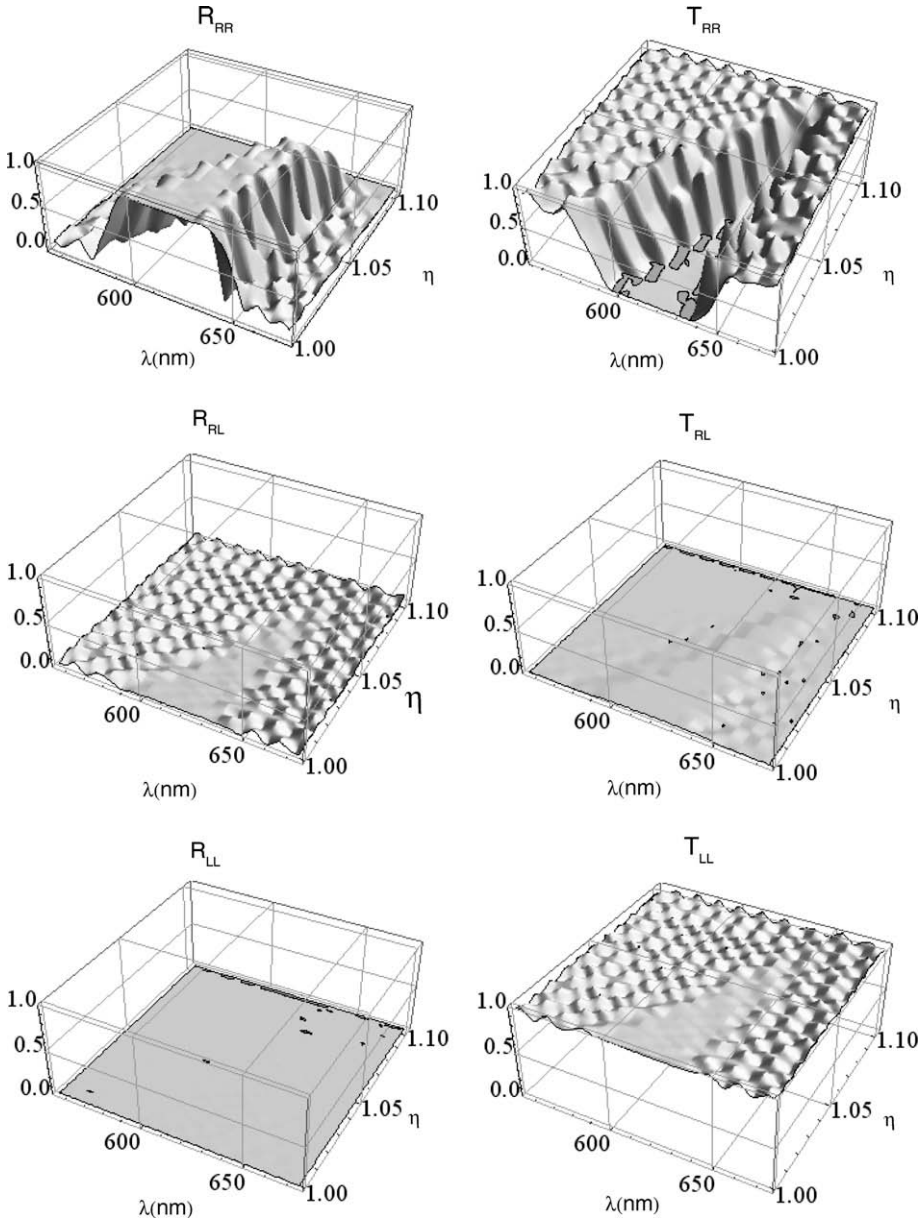


**Fig. 4.** Transmittances and reflectances as a function of the wavelength $\lambda$ and the axial elongation $\eta$ for normal incidence.

tion of the incidence angles $\theta$ an $\varphi$, the axial elongation $\eta$, and the wavelength $\lambda$.

### 3.2. Matrix representation

Curl Maxwell equations in SI units are given by

$$\nabla \times \mathbf{E} = \mathrm{i}\omega\mu_o \mathbf{H}, \tag{22}$$

$$\nabla \times \mathbf{H} = -\mathrm{i}\epsilon_o \omega \epsilon(z) \cdot \mathbf{E}, \tag{23}$$

where the $z$-dependent dielectric tensor of the elastomer, submitted to an axial stress, was determined in Section 2. The general solutions for the above equations without any loss of generality can be written as

$$\mathbf{E}(r,t) = \mathrm{e}^{\mathrm{i}(\mathbf{k}^t \cdot \mathbf{r} - \omega t)} \varepsilon(z), \tag{24}$$

$$\mathbf{H}(r,t) = \mathrm{e}^{\mathrm{i}(\mathbf{k}^t \cdot \mathbf{r} - \omega t)} \mathbf{h}(z), \tag{25}$$

where $\mathbf{k}^t = (k_o \sin\theta\cos\varphi, k_o \sin\theta \sin\varphi, 0)$ is the transverse wave vector with $k_o = \frac{2\pi}{\lambda}$ the wave number, $\lambda$ the vacuum wavelength, $\theta$ and $\varphi$ are the incidence angles, $\varepsilon(z) = (\varepsilon_x(z), \varepsilon_y(z), \varepsilon_z(z))$ and $\mathbf{h}(z) = (h_x(z), h_y(z), h_z(z))$ are electric and magnetic amplitudes in the elastomer slab.

After substituting Eqs. (24) and (25) into Maxwell equations we find a set of equations which only depend on $z$. We solve them for $\varepsilon_z(z)$ and $h_z(z)$ in terms of the remaining components to obtain a system only for the transverse components of the fields which can be expressed as the matrix first order equation [16]

$$\frac{\mathrm{d}}{\mathrm{d}z} \boldsymbol{\Psi}(z) = -\mathrm{i}\mathbf{M}(z) \cdot \boldsymbol{\Psi}(z), \tag{26}$$

where

$$\boldsymbol{\Psi}(z) = \begin{pmatrix} \varepsilon_x(z) \\ \varepsilon_y(z) \\ h_x(z) \\ h_y(z) \end{pmatrix}. \tag{27}$$

Here the $4 \times 4$ matrix is defined as

$$\mathbf{M}(z)=\begin{pmatrix} \frac{k_x^t\epsilon_{zx}}{\epsilon_{zz}} & \frac{k_x^t\epsilon_{zy}}{\epsilon_{zz}} & -\frac{k_x^tk_y^t}{\zeta\epsilon_{zz}} & \frac{k_x^{t2}}{\zeta\epsilon_{zz}}-\beta \\ \frac{k_y^t\epsilon_{zx}}{\epsilon_{zz}} & \frac{k_y^t\epsilon_{zy}}{\epsilon_{zz}} & \beta-\frac{k_y^{t2}}{\zeta\epsilon_{zz}} & \frac{k_x^tk_y^t}{\zeta\epsilon_{zz}} \\ \frac{k_x^tk_y^t}{\beta}-\frac{\epsilon_{yz}\epsilon_{zx}\zeta}{\epsilon_{zz}}+\epsilon_{yx}\zeta & \epsilon_{yy}\zeta-\frac{k_x^{t2}}{\beta}-\frac{\epsilon_{yz}\epsilon_{zy}\zeta}{\epsilon_{zz}} & \frac{k_y^t\epsilon_{yz}}{\epsilon_{zz}} & -\frac{k_x^t\epsilon_{yz}}{\epsilon_{zz}} \\ \frac{k_y^{t2}}{\beta}+\frac{\epsilon_{xz}\epsilon_{zx}\zeta}{\epsilon_{zz}}-\epsilon_{xx}\zeta & \frac{\epsilon_{xz}\epsilon_{zy}\zeta}{\epsilon_{zz}}-\frac{k_x^tk_y^t}{\beta}-\epsilon_{xy}\zeta & -\frac{k_y^t\epsilon_{xz}}{\epsilon_{zz}} & \frac{k_x^t\epsilon_{xz}}{\epsilon_{zz}} \end{pmatrix}, \tag{28}$$

where $k_i^t$ $(i=x,y)$ denotes the $i$ component of the transverse wave vector $\mathbf{k}^t$, and $\epsilon_{mn}$ $(n,m=1,2,3)$ represent the elements of the dielectric tensor $\boldsymbol{\epsilon}$, $\zeta=\epsilon_o\omega.$ and $\beta=\mu_o\omega.$

### 3.3. The Oseen transformation

The differential system given by Eq. (26) can be solved using a numerical integration. Nevertheless, it is possible to find a reference system, for a normally incident wave, for which the solution can be obtained analytically. This has been done for SCM [7], using the Oseen transformation [17], where the reference system rotates along the $z$-axis in the same way as the director $\hat{\mathbf{n}}$.

For oblique incidence, let us define a new vector as

$$\boldsymbol{\Psi}'(z)=\mathbf{G}(z)\cdot\boldsymbol{\Psi}(z), \tag{29}$$

where

$$\mathbf{G}(z)=\begin{pmatrix} \cos qz & \sin qz & 0 & 0 \\ -\sin qz & \cos qz & 0 & 0 \\ 0 & 0 & \cos qz & \sin qz \\ 0 & 0 & -\sin qz & \cos qz \end{pmatrix}. \tag{30}$$

Substituting the above equation into the differential system Eq. (26), we obtain

$$\frac{\mathrm{d}}{\mathrm{d}z}\boldsymbol{\Psi}'(z)=-\mathrm{i}\mathbf{M}'(z)\cdot\boldsymbol{\Psi}'(z), \tag{31}$$

with

$$\mathbf{M}'(z)=\begin{pmatrix} \kappa\delta\cos u & \mathrm{i}q & \frac{\kappa^2\epsilon_d\sin 2u}{2\zeta\epsilon_\perp\epsilon_\parallel} & \frac{\kappa^2\epsilon_d\cos^2 u}{\zeta\epsilon_\perp\epsilon_\parallel}-\beta \\ -\mathrm{i}q-\kappa\delta\sin u & 0 & \beta-\frac{\kappa^2\epsilon_d\sin^2 u}{\zeta\epsilon_\perp\epsilon_\parallel} & -\frac{\kappa^2\epsilon_d\sin 2u}{2\zeta\epsilon_\perp\epsilon_\parallel} \\ -\frac{\kappa^2\sin 2u}{2\beta} & \zeta\epsilon_\parallel-\frac{\kappa^2\cos^2 u}{\beta} & 0 & \mathrm{i}q \\ \frac{\kappa^2\sin^2 u}{\beta}-\zeta\epsilon_d & \frac{\kappa^2\sin 2u}{2\beta} & \kappa\delta\sin u-\mathrm{i}q & \kappa\delta\cos u \end{pmatrix}, \tag{32}$$

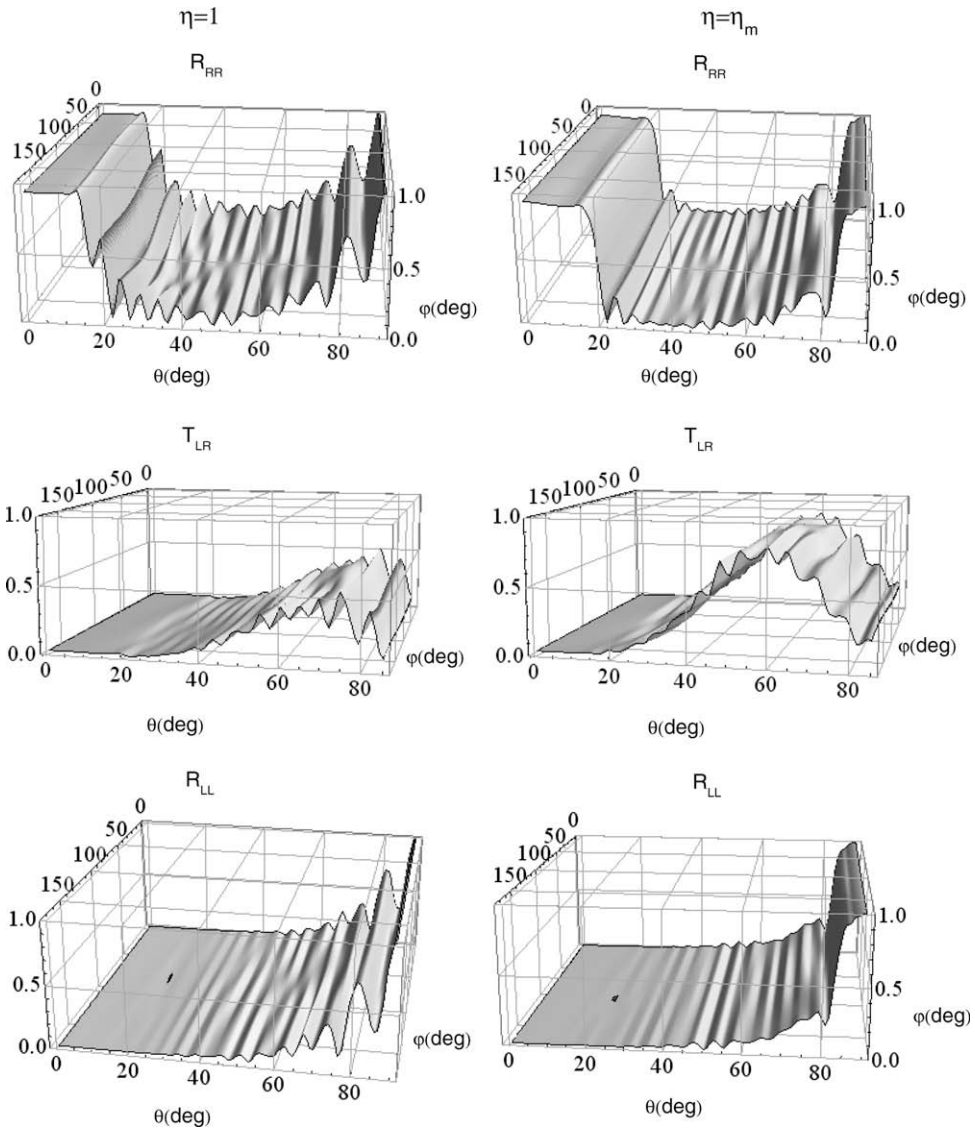


**Fig. 5.** Reflectances as a function of the angles $\theta$ and $\varphi$ for $\lambda=500$ nm.

where we have introduced the abbreviations

$$u = qz - \varphi \tag{33}$$

$$\kappa = k_o \sin\theta, \tag{34}$$

$$\epsilon_d(\eta) = \frac{\epsilon_\perp \epsilon_\parallel}{\epsilon_\perp \sin^2\alpha(\eta) + \epsilon_\parallel \cos^2\alpha(\eta)}, \tag{35}$$

$$\delta(\eta) = \frac{\epsilon_d \epsilon_a \sin 2\alpha(\eta)}{2\epsilon_\perp \epsilon_\parallel}. \tag{36}$$

In general, $\mathbf{M}'(z)$ is $z$-dependent but for normal incidence, $\theta = 0$, it is not and reduces to

$$\mathbf{M}'_o = \begin{pmatrix} 0 & iq & 0 & -\beta \\ -iq & 0 & \beta & 0 \\ 0 & \zeta\epsilon_\perp & 0 & iq \\ -\zeta\epsilon_d(\eta) & 0 & -iq & 0 \end{pmatrix}, \tag{37}$$

and as a consequence Eq. (26) can be solved analytically. The eigenvalues of $\mathbf{M}'_o$ are given by

$$k_{1,2}^2 \equiv q^2 + \frac{1}{2}(\epsilon_d(\eta) + \epsilon_\perp)\zeta\beta \mp \frac{1}{2}\sqrt{\zeta\beta(8q^2(\epsilon_d(\eta) + \epsilon_\perp) + (\zeta\beta)^2(\epsilon_d(\eta) - \epsilon_\perp)^2)}. \tag{38}$$

Only the modes $k_1^\pm$ show a bandgap for $\omega$ within the interval defined by the positive roots of the equation $k_1^2 = 0$ whose corresponding wavelengths are given by

$$\lambda_1 \equiv \frac{2\pi\eta}{q_o}\sqrt{\epsilon_\perp}, \quad \lambda_2 \equiv \frac{2\pi\eta}{q_o}\sqrt{\epsilon_d(\eta)}. \tag{39}$$

In this interval $k_1^\pm$ are pure imaginary and their corresponding eigenvectors are linearly polarized. Thus, the central wavelength of the bandgap is

$$\lambda^C = \frac{\lambda_1 + \lambda_2}{2} = \frac{p\eta\sqrt{\epsilon_\perp}}{2}\left(1 + \sqrt{\frac{\epsilon_\parallel}{\epsilon_\perp + \epsilon_a \frac{(\eta^{3/2}-1)}{(r-1)}}}\right), \tag{40}$$

where we have substituted in this expression Eqs. (7) and (35). Eq. (40) demonstrates clearly that for a positively anisotropic elastomer, the reflected wavelength $\lambda^C$ increases by stretching the sample along the helix axis. This behavior is in qualitative agreement with the biaxial extension experiments performed by Finkelmann et al. [18] in which $\lambda^C$ decreases due to an effective compression along the helix axis.

The general solution for oblique incidence, $\theta \neq 0$, can be written formally as $\mathbf{\Psi}'(z) = \mathbf{\Psi}'(0) \cdot \mathbf{Mt}(z)$, where $\mathbf{Mt}(z) = e^{\int_o^z \mathbf{M}'(z')dz'}$. Here $\mathbf{Mt}(z)$ can be determined using a numerical procedure based on the piecewise constant approximation for which it is useful to take advantage of the periodicity of $\mathbf{Mt}(z)$ to optimize the algorithm.

Since $\mathbf{\Psi}'(z)$ lies in the Oseen reference system we need to transform it back to the laboratory system. Hence, the solution in the original reference system is

$$\mathbf{\Psi}(L) = \mathbf{U} \cdot \mathbf{\Psi}(0), \tag{41}$$

where the transfer matrix $\mathbf{U}$ is given by $\mathbf{U} = \mathbf{G}^T(L) \cdot \mathbf{Mt}(L) \cdot \mathbf{G}(0)$. Here the superscript T denotes the transpose conjugated of the matrix.

## 4. Results and conclusions

The material parameters we use to perform the calculations are: $r = 1.16$, $L = 10.7\ \mu m$, $\frac{p}{2} = 214\ nm$, $\epsilon_\perp = 1.91$, $\epsilon_\parallel = 2.22$, $\mu = 1$ which correspond to a real sample made by a siloxane backbone chain reacting with 90 mol% and 10% of the flexible difunctional cross-linking groups (di-11UB). The rod like mesogenic groups are present in the proportion 4:1 between the nematic 4-pentylphenyl-4′-(4-buteneoxy) benzoate (PBB) and the derivative of chiral cholesterol pentenoate (ChP) [19]. In Figs. 2 and 3 we show the co-polarized and cross-polarized transmittances and reflectances as a function of $\lambda$ and $\theta$. In the first column, we set $\eta = 1$, which is equivalent to have an elastomer under no deformation, whereas in the second column we use $\eta_m = 1 + \frac{\eta_M - 1}{2} = 1.052$ for which the system is submitted to half of its critical elongation.

Notice that Figs. 2 and 3 are consistent with the usual circular Bragg phenomenon for which the right circularly polarized wave impinging a right-handed elastomer, is highly reflected, while the left circularly polarized wave is transmitted. The center of the bandgap blue-shifts as a the incidence angle increases, as it occurs in the absence of stress.

We also observe that by increasing the elongation, the bandwidth decreases as can be seen by comparing the right- and the left-hand columns of Figs. 2 and 3. Moreover, when the strain is the critical $\eta_M = 1.16^{2/3} = 1.1040$, the bandgap disappears due to the fact the cholesteric director is completely aligned with the helical axis as can be observed from Fig. 4. This effect opens up the door for proposing novel devices to mechanically control the light flow, since it allows to switch off a bandgap by applying a mechanical stress to the elastomer. This is clearly illustrated in Fig. 4 where the bandwidth diminishes as a function of the deformation for normal incidence.

Fig. 5 displays the reflectances against $\theta$ and $\varphi$ for $\lambda = 630$ nm. We notice a band reflection for $R_{RR}$ between $\theta = 30^\circ$ and $\theta = 40^\circ$ which displaces for larger angles as $\eta$ gets larger. On the other hand, $R_{LR}$ diminishes in 25% by spreading its oscillations to almost every $\theta$-value. Also, $R_{LL}$ widens its starting flat region for larger angles.

In summary, we have calculated the transmittances and reflectances of an electromagnetic wave impinging an elastomer under the influence of a mechanical strain parallel to the helical axis. We have shown that the circular Bragg phenomenon can be mechanically controlled by the application of a mechanical stress in such way that can alter the bandwidth and even switch off the bandgap when the strain takes the critical value $\eta_M$. We have shown that under the presence of an elongation the bandgap blue-shifts as $\theta$ increases in similar way as happens in the absence of deformation.

These results show that it is possible to mechanically control the circular Bragg phenomenon for tuning and switching applications. Finally we have shown analytically that the reflected wavelength $\lambda^C$ at normal incidence red-shifts by stretching the elastomer along the helix axis. We expect that our results motivate the development of optical devices based on elastomers and activated by an elongation.

## References

[1] H.A. Macleod, Thin-Film Optical Filters, third ed., Institute of Physics Publishing, Bristol, 2001.
[2] P.G. de Gennes, J. Prost, The Physics of Liquid Crystals, second ed., Clarendon Press, Oxford, 1993 (Chapter 6).
[3] C.G. Avendaño, S. Ponti, J.A. Reyes, C. Oldano, J. Phys. A Math. Gen. 38 (2005) 8821.
[4] A. Lakhtakia, R. Messier, Sculptured Thin Films: Nanoengineered Morphology and Optics, SPIE Press, Washington, 2005 (Chapter 9).
[5] M. Warner, E.M. Terentjev, Liquid Crystals Elastomers, Clarendon Press, Oxford, 2003 (Chapter 9).
[6] D.A. Pinnow, R.L. Abrams, J.F. Lotspeich, D.M. Henderson, T.K. Plant, R.R. Stephens, C.M. Walker, Appl. Phys. Lett. 34 (1979) 391.
[7] J.A. Reyes, A. Lakhtakia, Opt. Commun. 259 (2006) 164.
[8] J.A. Reyes, A. Lakhtakia, Opt. Commun. 266 (2006) 565.
[9] S. Kim, H. Finkelmann, Marcromol. Rapid Commun. 2 (1981) 317.
[10] A. Komp, J. Rühe, H. Finkelmann, Macromol. Rapid Commun. 26 (2005) 813.

[11] J. Schmidtke, S. Kniesel, H. Finkelmann, Macromolecules 38 (2005) 1357.
[12] M. Rivera, J.A. Reyes, Appl. Phys. Lett. 90 (2007) 023513.
[13] S. Chandrasekhar, Liquid Crystals, Cambridge University Press, Cambridge, 1997.
[14] Y. Mao, E.M. Terentjev, M. Warner, Phys. Rev. E 64 (2001) 041803.
[15] J.D. Jackson, Classical Electrodynamics, Wiley, New York, 1975.
[16] N. Marcuvitz, J. Schwinger, J. Appl. Phys. 22 (1951) 806.
[17] C.W. Oseen, Trans. Faraday Soc. 29 (1933) 883.
[18] H. Finkelmann, S.T. Kim, A. Muñoz, P. Palffy Muhoray, B. Taheri, Adv. Mater. 13 (2001) 1069.
[19] P. Cicuta, A.R. Tajbakhsh, E.M. Terentjev, Phys. Rev. E 65 (2002) 051704.